JURNAL GEOGRAFI
https://journal.unnes.ac.id/nju/index.php/JG

Analysis of Hail Based on Atmospheric Conditions and Himawari-9 Satellite: Case Study of Surabaya City, March 20, 2023

Imawan Mashuri[1*], Sayful Amri[2], Fadhli Aslama Afghani[3], Fadhil Muhammad Aslam[4]

[1,2,3,4]Department of Climatology, State College of Meteorology Climatology and Geophysics, Tangerang City, Indonesia

Article Info

Article History
Submitted 2025-03-03
Revised 2025-06-01
Accepted 2025-06-11

Keywords
Atmospheric, Hail, Himawari-9 Satellite, Surabaya

Abstrak

Hujan es merupakan fenomena cuaca ekstrem yang jarang terjadi di Indonesia. Pada 20 Maret 2023, hujan es terjadi di Kota Surabaya. Penelitian ini dilakukan untuk menganalisis hujan es berdasarkan kondisi atmosfer dan satelit Himawari-9. Analisis skala global menunjukkan adanya anomali suhu permukaan laut di Samudra Hindia Tenggara. Secara regional, adanya garis geser monsun dan transportasi uap air lapisan rendah yang signifikan dari Laut Jawa Selatan menyebabkan konvergensi di Surabaya. Secara lokal, terjadi peningkatan kelembapan relatif sebesar 10% serta penurunan suhu permukaan sebesar 3,2°C, yang mengakibatkan kondisi permukaan yang lebih lembap. Kondisi lapisan udara atas juga mendukung terjadinya hujan es, di mana empat indeks (CAPE, LI, TT, dan SWEAT) berada dalam kategori sedang. Sebaliknya, CIN berada dalam kategori rendah, dan KI mengalami pergeseran dari kategori sedang ke tinggi. Indeks CAPE kategori sedang pada lapisan menengah dari arus naik udara lembap berkontribusi terhadap terbentuknya hujan es dengan ukuran maksimum. Awan mencapai tingkat pembekuan di atmosfer lapisan menengah pada ketinggian 5048 meter dan 4776 meter. Teknik RGB Day Microphysics dengan citra satelit Himawari-9 mengidentifikasi puncak awan yang menembus lapisan atmosfer serta penurunan drastis suhu puncak awan hingga -82,5°C, yang menunjukkan adanya pergerakan udara ke atas yang kuat serta pembentukan awan konvektif yang melampaui tingkat pembekuan.

Abstract

Hail is a rare extreme weather phenomenon in Indonesia. On March 20, 2023, hail occurred in Surabaya City. The research was conducted to analyze the hail based on atmospheric conditions and the Himawari-9 satellite. Analysis of the global scale showed anomalies in sea surface temperature in the Southeast Indian Ocean. Regionally, a monsoon shear line and significant low-level moisture transport from the South Java Sea caused convergence in the Surabaya. Locally, there was a significant increase in relative humidity by 10%, and a surface temperature decrease of 3.2°C resulted in wetter surface weather. The occurrence of hail was also supported by upper air conditions, with four indices (CAPE, LI, TT, and SWEAT) falling within the moderate category. In contrast, CIN was categorized as low, while KI increased from moderate to high. A moderate CAPE index in the mid-level updraft of moist air resulted in the maximum hail size. Clouds reached the freezing level in the mid-level atmosphere at 5048 meters and 4776 meters. The RGB Day Microphysics technique using Himawari-9 satellite imagery identified overshooting tops and a drastic decrease in top cloud temperature reaching -82.5°C, indicating the presence of a strong updraft and the formation of convective clouds that surpassed the freezing level.

E-mail: imawanmashuri19@gmail.com

p-ISSN 2549-3078 e-ISSN 2549-3094

INTRODUCTION

The phenomenon of hail occurred in Surabaya City on March 20, 2023 (Achmad Faizal, 2023). The event occurred at 07:30 UTC or 14:30 local time (Abdulhakim, 2023). Hail events are commonly noticed primarily during the period leading up to the monsoon season, occurring typically from March to April in the country (Auliya & Mulya, 2022; Hidayat et al., 2017; Kristianto et al., 2018). The Indonesian Agency for Meteorological, Climatological, and Geophysics (BMKG) classifies hail as an extreme weather phenomenon (BMKG, 2010). The impacts of hail include damaging infrastructure such as roof tile and glass, reducing agriculture, and impeding human activities (Al-Bagawi et al., 2021; Punge & Kunz, 2016; Wapler, 2017; Williams-Linera et al., 2023).

Hail is a form of precipitation consisting of irregularly shaped ice pellets with a diameter of about 5 mm, formed from Cumulonimbus clouds (Tjasyono, 2004). Hail typically occurs in extra-tropical regions due to a lower freezing level (Fadholi, 2012). When the cloud has grown beyond the freezing point, extremely cold water particles will freeze into ice particles. Strong wind shear supports surface hailfall by tilting updrafts in convective clouds (Beal et al., 2020). Hail phenomena occur when thunderstorm clouds or Cumulonimbus clouds (CB) with higher updraft speeds, facilitate the formation of many ice particles (Houze, 1993; Kunz et al., 2020). Several previous studies have shown the existence of overshooting tops in convective clouds during hail events (Paski et al., 2017; Sanjaya & Amri, 2022). However, it has not analyzed the stability conditions in the upper air and the distribution of hail or precipitation.

Understanding the environmental conditions leading to hail formation is crucial for improving early warning systems and minimizing potential impacts. The development of hailstorms is influenced by various atmospheric factors, including temperature, humidity, wind patterns, and vertical instability (Dessens, 1995; Rasmussen & Heymsfield, 1987). In tropical regions such as Indonesia, hail is relatively rare due to higher freezing levels, but extreme convective activity can still trigger its occurrence (Trapp et al., 2007). Analyzing meteorological parameters, such as convective available potential energy (CAPE) and vertical wind shear, can provide insights into the dynamics of hail-producing storms.

The characteristics of hail, such as its shape, size, mass, and internal structure, are interrelated through microphysical growth processes (Allen et al., 2020). One approach for examining microphysical growth involves the utilization of Himawari-9 satellite imagery. Developed by the Japan Meteorological Agency (JMA), this satellite provides significant observational capabilities to assist users in enhancing and refining various physical products such as convective cloud detection and cloud genesis (Bessho et al., 2016). Unlike NOAA's polar-orbiting satellites that pass over the same area only twice a day, Himawari's geostationary position enables continuous monitoring every 10 minutes (Schmit et al., 2017). Consequently, the objective of the research is to analyze hail phenomena in Surabaya City based on atmospheric conditions and Himawari-9 satellite imagery.

METHODS

The research was located in Surabaya City with astronomical coordinates of 7°09′– 7°21′ South Latitude and 112°36′–112°54′ East Longitude. Surabaya City consists of 31 districts, with some districts experiencing hail, such as the Pakal, Tandes, and Benowo. The time for carrying out this research on March 20, 2023. For further detail, the research location on Figure 1.

The study used SATAID (SATellite Animation and Interactive Diagnosis) to interactively observe cloud development, as it effectively highlights convective cloud features and temporal weather changes (JMA, 2018). GrADS (Grid Analysis and Display System) was also used to analyze meteorological parameters, given its strength in processing gridded data and generating time-series visualizations (Doty & Kinter, 1995). The combination of these tools allows for a comprehensive, multi-scale analysis of the atmospheric dynamics leading to the hail event. The materials for research using Himawari-9 image data include Band-4, Band-7, and Band-13. The other Meteorological data utilized were:

1. Observation and upper air (radiosonde) data from Juanda Meteorological Station.
2. NOAA reanalysis data at 0.25° × 0.25° global grid (Reynolds et al., 2007), with Sea Surface Temperature Anomaly parameter.
3. ERA5 hourly reanalysis data at a resolution of 0.25° × 0.25° provided by ECMWF (Hersbach et al., 2020), includes U-component of wind, V-component of wind, and specific humidity.
4. GSMap precipitation data with high temporal (hourly) and 0.1° × 0.1° spatial resolution (Darand & Siavashi, 2021).

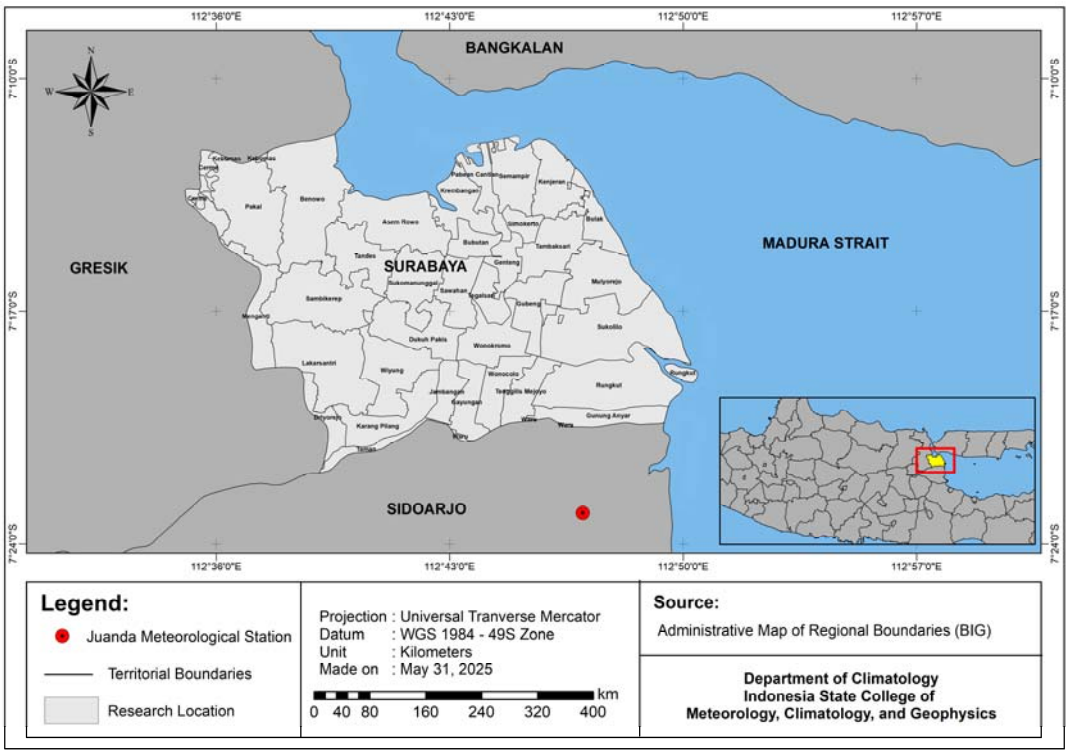

Figure 1. Research Location Map

The research uses a case study approach to investigate the atmospheric conditions that led to a hail event. In this study, Surabaya was chosen as the case due to the occurrence of a rare hail phenomenon in the city. Analysis of atmospheric conditions is conducted sequentially based on different weather factors and scales, such as global, regional, and local.

The regional weather factors under analysis include the streamlining of gradient wind, LLMT (Low-Level Moisture Transport), and divergence of LLMT. The streamline of gradient wind was generated using ERA5 reanalysis data with the U-component of wind and V-component of wind at 925 hPa pressure level. The equation of gradient wind is

$$\frac{V_{gr}^2}{R} = f_o V_{gr} - f_o V_g = 0 \quad (1)$$

V_{gr} represents gradient wind; R stands for the radius of curvature of wind trajectories; f_o is the Coriolis parameter (Gold, 1908). In addition, the streamlines are determined by the integration of

$$\frac{dy}{dx} = \frac{u(x,y,t_0)}{v(x,y,t_0)} \quad (2)$$

in relation to x at time t_0 (Holton, 1992). The data used to create Low-Level Moisture Transport (LLMT) involved ERA5 reanalysis data for the U-component of wind and the V-component of wind, and specific humidity at the 850–1000 hPa pressure level.

The mathematical equation to calculate low-level moisture transport is

$$\vec{Q} = \frac{1}{g}\int_{850}^{1000} q\vec{V}dP \quad (3)$$

$\vec{Q}$ representing moisture transport (kg/ms); q being specific humidity; g denoting gravitational acceleration (m/s^2); $\vec{V}$ being the horizontal wind vector (Lélé et al., 2015). The divergence of LLMT is an indicator of water vapor sources and sinks which represents the net moisture transport (Chen et al., 1988). The mathematical equation to calculate the divergence of LLMT is

$$\nabla^2 \bar{x} = E - P \quad (4)$$

which, E is evaporation from the surface and P is precipitation (d'Abreton & Tyson, 1995).

The local weather factors under analysis include synoptic and upper air conditions, time series and contour of cloud-top temperature, spatial pattern of cloud, and spatial pattern of precipitation. The synoptic conditions encompassed surface temperature, surface pressure, relative humidity, wind speed, and wind direction, whereas the upper air conditions such as the height of the freezing level, Convective Available Potential Energy (CAPE), Convective Inhibition (CIN), Lift Index (LI), K-Index (KI), Total-Totals Index (TT), and Severe Weather Threat Index (SWEAT).

These observational data aimed to provide insights into surface weather and upper air during the Hail event.

Table 1. Categorize of the Atmospheric Instability Index

Index	Low	Moderate	High
CAPE	<1000	1000 to 2500	>2500
CIN	>10	10 to 100	<10
LI	>-2	-2 to -6	<-6
KI	<29	29 to 37	>37
TT	<42	42 to 46	>46
SWEAT	<135	135 to 239	>239

Source: (Fibriantika & Mayangwulan, 2020; Wirjohamidjojo & Swarinoto, 2014)

Red Green Blue (RGB) technique of SATAID employed in the analysis of the spatial pattern of the cloud is Day Microphysics. The main application of Day Microphysics is to manifold cloud analysis such as temperature, cloud optical thickness, cloud particle phase, and size. The benefit of RGB Day Microphysics is its usefulness in identifying Cumulonimbus Cloud (Cbs) with small ice particles, water clouds, and super-cooled water clouds (JMA, 2018). Channel IR1 (Band 13) data were employed to generate a contour and time-series graph depicting the temperature at the top of the clouds (Kristianto et al., 2018). The spatial pattern of precipitation is plotted using GrADS with hourly data from GSMaP.

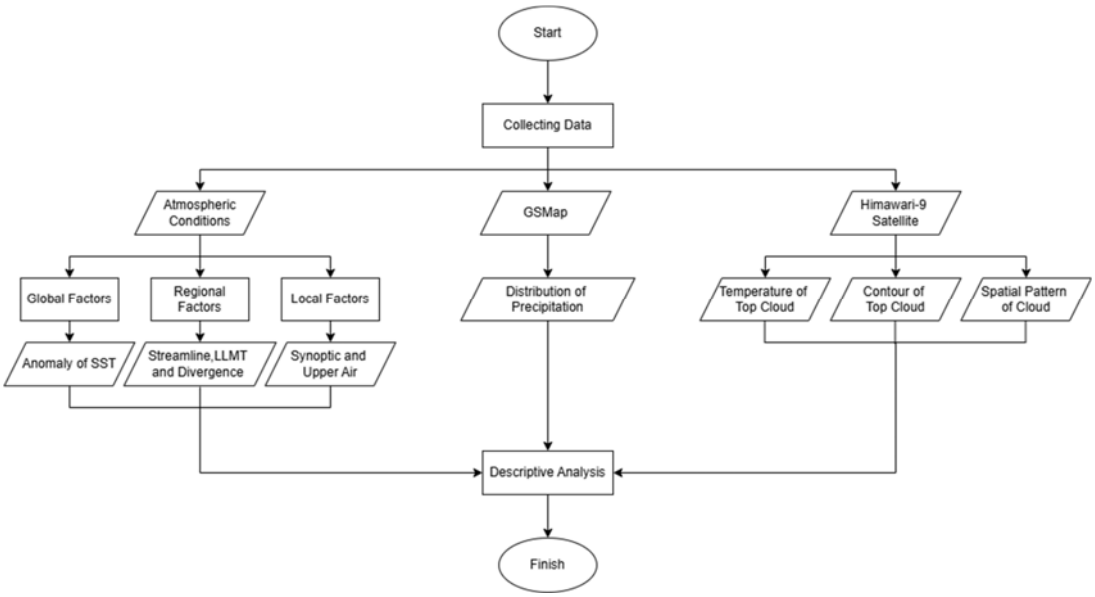

Figure 2. Research Flowchart

RESULT AND DISCUSSION

1. Global Factor: Sea Surface Temperature Anomaly

Indonesia, especially the city of Surabaya is situated in the equatorial region. It receives sunlight throughout the year, resulting in consistently high sea surface temperatures compared to the high-latitude region. There was an anomaly of sea surface temperature on March 20, 2023, in the Southeast Indian Ocean ranging from -0.9°C to 2.7°C and North Java Sea ranging from -1.2°C to 1.5°C. During the period from March to May (MAM), a transition towards the summer season occurs (Tokinaga & Tanimoto, 2004), marked by an increase in sea surface temperatures and changes in weather patterns (increase precipitation) across Indonesia area, especially Surabaya City (Hasibuan et al., 2024). For further details, refer to Figure 3.

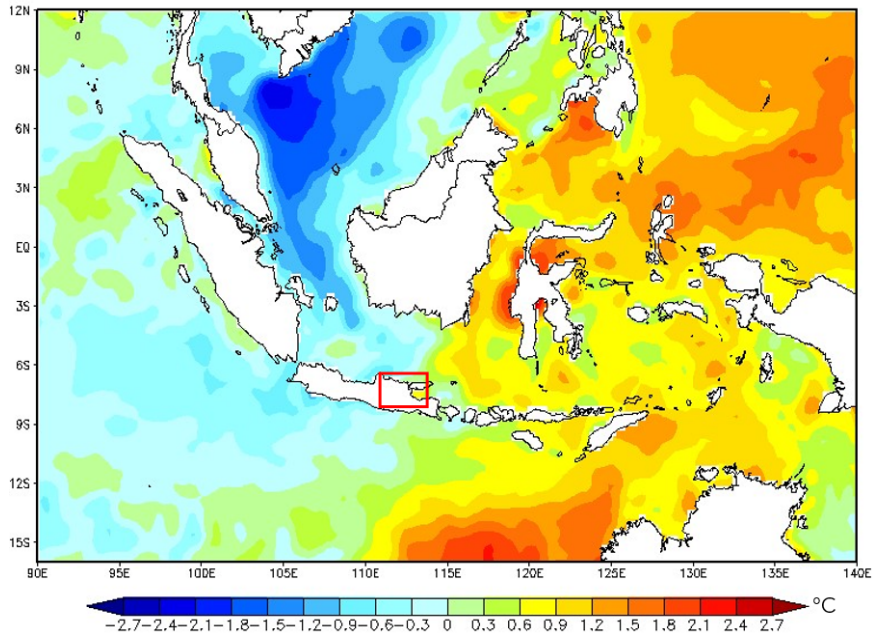

Figure 3. Daily of Sea Surface Temperature Anomaly

2. Regional Factors: Streamline of Gradient Wind, Low-level Moisture Transport (LLMT), and Divergence of LLMT

There are two prevailing winds evident in the streamline map, namely the Australian monsoon wind affecting the southern part of Java Island and the Asian monsoon wind influencing the northern part of Java Island (Haryanto et al., 2020; Tjasyono, 2006). During this period, a transitional phase occurs as the Asian monsoon weakens, whereas the Australian monsoon begins to strengthen marking a shift in seasonal wind patterns over the region.

The analysis of gradient wind reveals the presence of a monsoon shear line around Surabaya City on March 20, 2023, at 07:00 UTC. The monsoon shear line causes a slowdown in the airflow, resulting in the buildup of water vapor (McBride & Keenan, 1982). This accumulation of water vapor eventually triggers the formation of convective clouds in the surrounding area of the shear line (Bao & Yao, 2022; Xiu-ping et al., 2020). The wind speed on the shear line is measured around from 3 knot to 9 knot. The shearline responsible for heavy rainfall exhibits a lower speed in contrast to the shearline inducing hail (Tuovinen et al., 2015). For further details, refer to Figure 4.

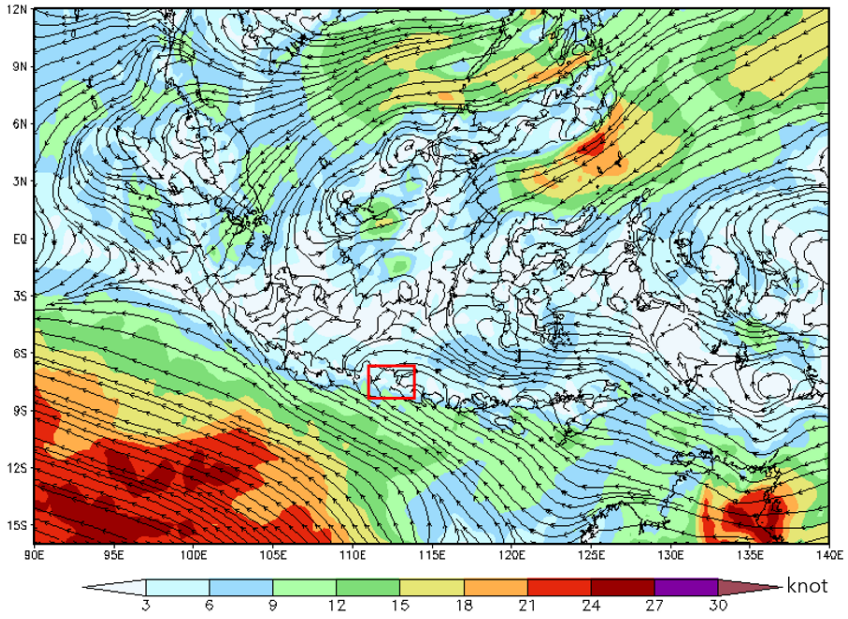

Figure 4. Streamline of Gradient Wind at 00 UTC

The analysis of Low-Level Moisture Transport (LLMT) indicates the dominance of moisture transport from the South Java Sea (Indian Ocean) towards Java Island, including the city of Surabaya. The pattern of moisture transport follows the gradient wind streamline, moving from the southeast toward the northwest (zonal transport). The low-level moisture transport moving towards Surabaya City appears in soft blue with a value of around 30 kg/ms at 07 UTC, whereas around 80 kg/ms at 08 UTC. The presence of low-level moisture transport can enhance the potential for precipitation and hail events in the city of Surabaya. For further details, refer to Figure 5.

The analysis of gradient wind reveals the presence of a monsoon shear line around Divergence analysis of Low-Level Moisture Transport (LLMT) indicates red shades within the range of values from -4°C to -9°C, both at 07 UTC and 08 UTC. This suggests the occurrence of convergence in the lower atmosphere to trigger the process of cloud formation (Ni'amillah et al., 2021). The persistence of these negative divergence values suggests sustained moisture convergence, potentially contributing to the development of deep convection and precipitation. Additionally, the surrounding areas with positive divergence reflect regions where moisture is being transported away. For further details, refer to Figure 6.

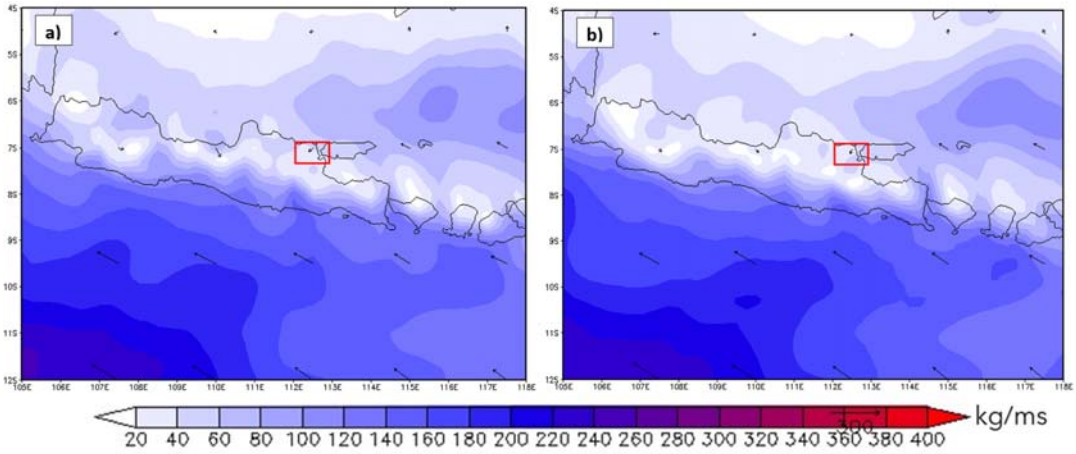

Figure 5. Low-Level Moisture Transport at a) 07 UTC b) 08 UTC

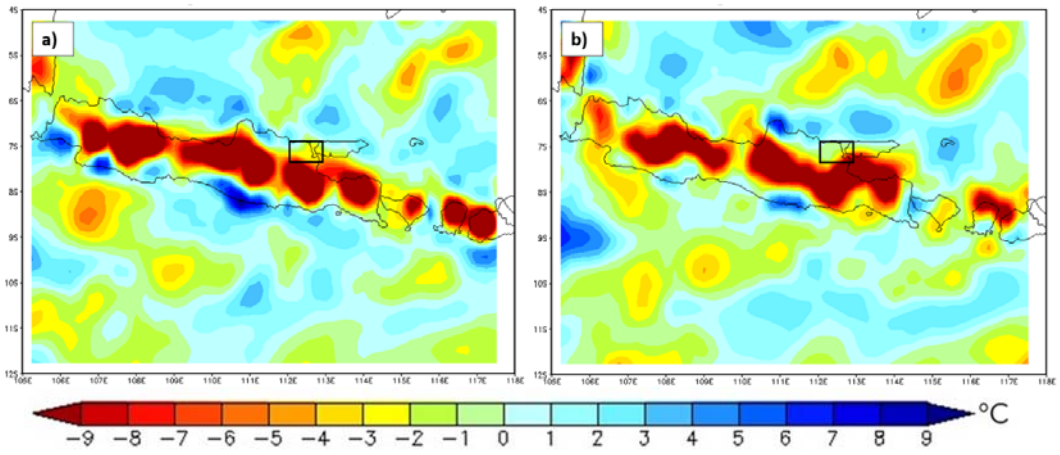

Figure 6. Divergence of Low-Level Moisture Transport at a) 07 UTC b) 08 UTC

3. Local Factors: Synoptic and Upper Air

The surface weather conditions before the hail event, are from 00:00 to 06:00 UTC. There was a continuous increase in surface temperature every hour, while the relative humidity decreased continuously every hour. On the other hand, the surface pressure wind speed, and wind direction exhibited fluctuating patterns.

At the time of the hail event occurrence precisely from 07:00 to 08.00 UTC, it was shown that the surface temperature had a significant decrease of 3.2°C, and surface pressure also declined by 0.1 mb. In contrast, the relative humidity was a significant increase of 10%. The precipitation led to the air becoming colder and more humid, resulting in a decrease in the surface temperature and an increase in relative humidity (Frystine et al., 2022). The wind was calm with a decrease of 7 knot.

After the hail event, the surface weather conditions from 09.00 to 12:00 UTC showed fluctuations in air temperature and relative humidity. However, air pressure increased continuously and the wind was calm. For further details, refer to Table 2.

Table 2. Synoptic Observation

Hour (UTC)	Surface Temperature (°C)	Surface Pressure (mb)	Relative Humidity (%)	Wind Speed 10 meters (knot)	Wind Direction 10 meters (From)
00.00	27.2	1009.5	87	2	North West
01.00	29.2	1009.9	79	0	Calm
02.00	31	1010.0	72	2	South East
03.00	32	1009.6	70	2	North
04.00	32	1009.1	68	7	North East
05.00	33	1008.4	64	7	North East
06.00	33.6	1007.1	61	2	North East
07.00	33.6	1007.0	59	7	South East
08.00	30.4	1006.9	69	0	Calm
09.00	29.3	1006.6	70	0	Calm
10.00	30.5	1007.1	94	0	Calm
11.00	28.8	1008.7	74	0	Calm
12.00	27.2	1009.8	89	0	Calm

Source: (Juanda Meteorological Station, 2023)

The analysis of upper air conditions can be conducted by utilizing radiosonde data generated by the Juanda Meteorological Station. Before the hail event at 00 UTC, the data indicates that the cloud reached the freezing level at an altitude of 5048 meters. The analysis of potential convective clouds with the CAPE index shows a value of 1448 J/kg, indicating the rapid growth of convective clouds and the likelihood of thunderstorms (Qian et al., 2019). The analysis of CIN index shows a value of -23.1 J/kg, indicating the low inhibiting force to parcel flow (Chakraborty et al., 2018). The analysis of air instability using the LI produces a value of -3.37°C, indicating an unstable lower troposphere condition relative to its upper part. The analysis of KI indicates the potential for thunderstorms with a value of 32.7°C, suggesting a thunderstorm potential of 60-80% (Prasetyo et al., 2020). The analysis of the TT index represents the area of development and strength of a thunderstorm (Ardiansyah, 2022), with a value of 44.4°C. The analysis of potential severe weather using the SWEAT Index yields a value of 228.3°C, indicating the likelihood of adverse weather due to convective activity.

After the hail event at 12 UTC, the data indicates that the convective cloud reached the freezing level at an altitude of 4776 meters, representing an upward movement toward the upper layers. The analysis of CAPE index reveals a value of 1582 J/kg, experiencing an increase of 134 J/kg. The analysis of CIN index reveals a value of -15 J/kg, experiencing an increase of 8.1 J/kg. The analysis of LI produces a value of -3.54°C, experiencing an increase of 0.17°C. The analysis of KI yields a value of 39.0°C, experiencing an increase of 6.3°C. The analysis of TT index Index yields a value of 45.7°C, experiencing an increase of 1.3°C. The analysis of SWEAT Index yields a value of 234.5°C, experiencing an increase of 6.2°C. Referring to Table 1, the four atmospheric instability indexes, such as CAPE, LI, TT, and SWEAT, fall into the moderate category, whereas CIN falls into the low category at both 00 UTC and 12 UTC. Moderate CAPE Index results in maximum hail sizes, due to the lateral movement through the midlevel updraft of moist inflow air originating from various source levels (Lin & Kumjian, 2022). The TT value undergoes a labile phase during the pre-monsoon period with a range of values between 45-50°C (Chakraborty et al., 2018). In contrast, the K-Index shifts from the moderate category to the low category, representing an increasing potential for thunderstorm formation. For further details, refer to Figure 7.

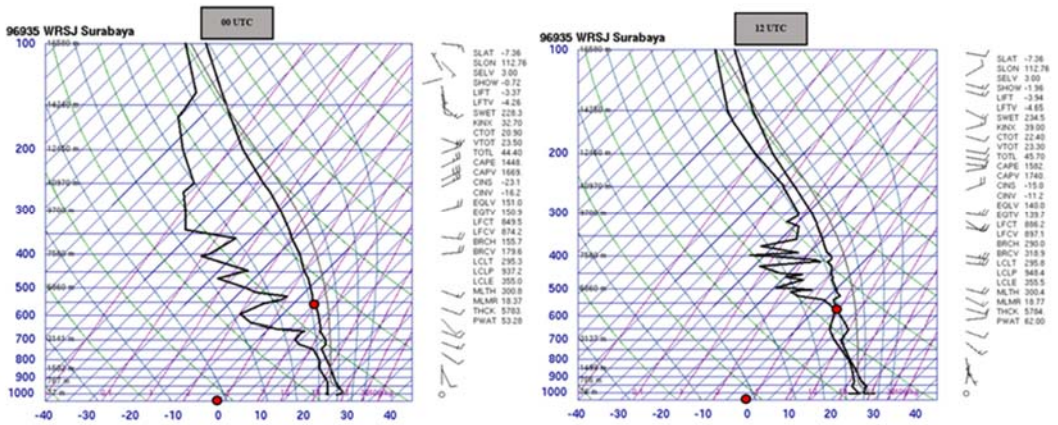

Figure 7. Skew-T Diagram of Radiosonde from Juanda Meteorogical Station

4. Satellite Information: Temperature, Contour, and Spatial Pattern of The Cloud

The temperature of the top cloud indicates the process of ice particle formation within convective clouds (Paski et al., 2017). Based on the time series analysis of Himawari-9 satellite images, it was shown that before the hail event from 00:00 UTC to 07:00 UTC, the temperature of the top cloud remained consistently at 20°C. The temperature of the top cloud started to decrease at 07:00 UTC, marking the initiation of convective cloud formation (cumulus stage).

During the occurrence of hail from 07:30 to 08:00 UTC, the temperature of the top cloud drastically dropped to -82.5°C. This condition indicates the formation of convective clouds that surpass the freezing level, leading to precipitation in the form of ice particles. After 08:00 UTC, the temperature of the top cloud began to rise again, simultaneous the hail ended. The temperature tends to fluctuate from 08.00 UTC to 14.00 UTC, ranging from -45°C to -60°C, representing the mature stage. The top cloud temperature returns from 14.00 UTC to 17.00 UTC, reaching 0°C (freezing level). The temperature increase is recognized as the dissipation stage of convective clouds (Auliya & Mulya, 2022). The orange color indicates the cumulus stage, the yellow color signifies the mature stage, and the green color indicates the dissipation stage. For further details, refer to Figures 8.

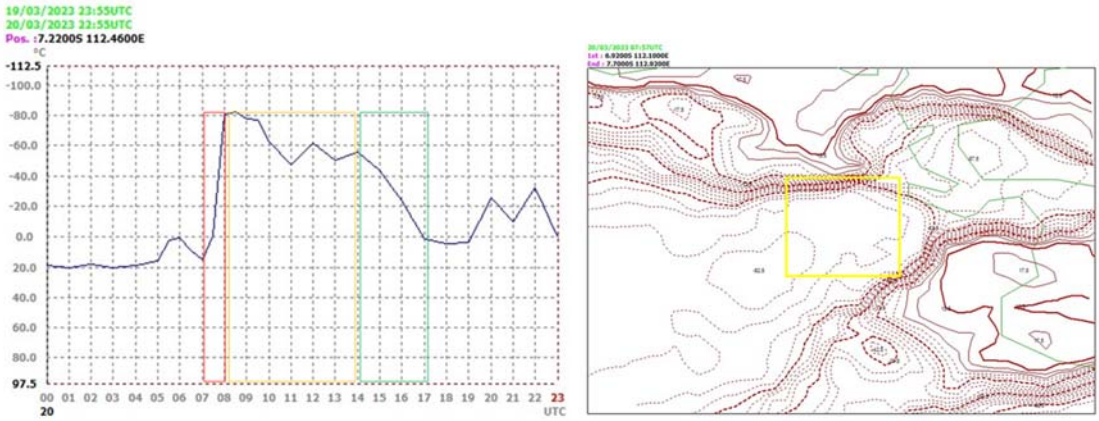

Figure 8. Time Series and Contour of Cloud-Top Temperature

The RGB Day Microphysics technique produces spatial cloud patterns during a hail event in the city of Surabaya. At 05:30 UTC, there was no apparent growth of convective clouds in all areas. By 06:30 UTC, signs of convective cloud growth began, but they had not yet moved into Surabaya City. At 07:30 UTC, there was a phase of convective cloud growth in the city of Surabaya. By 08:00 UTC, the convective clouds in the Surabaya region had reached a mature phase. During these 30 minutes, a change occurred where the clouds exhibited a rougher texture and bulging at the top, indicating the presence of an overshooting top. The presence of an overshooting top in convective clouds suggests the occurrence of a strong updraft, causing the convective clouds to penetrate the tropopause layer (Hassim, 2012; Jurković et al., 2015; Phoenix & Homeyer, 2021). At 08:30 UTC, convective clouds still covered Surabaya City with a smoother cloud texture, indicating the end of overshooting top activity. By 09:30 UTC, there was a dissipation phase of convective clouds characterized by a thinner coloration in Surabaya City. For further details, refer to Figure 9.

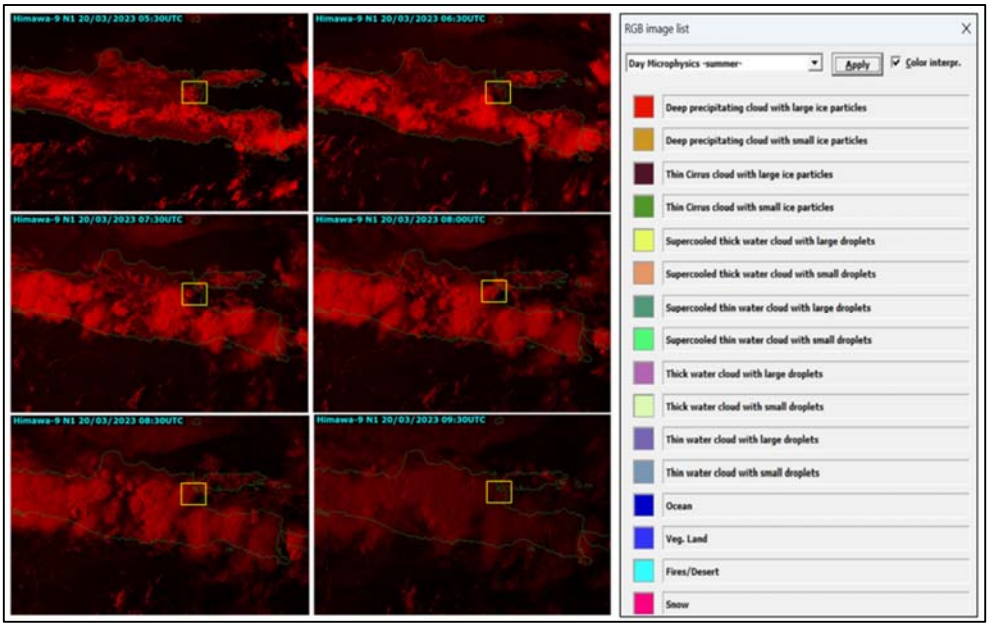

Figure 9. The Spatial Pattern of Cloud Using RGB Day Microphysics

5. The Distribution of Precipitation

Spatial analysis of precipitation indicates that the precipitation intensity at 07 UTC is 0 mm (no precipitation) in the eastern part of Surabaya, whereas ranges from 1-15 mm (moderate precipitation) in the western part of Surabaya. The distribution of precipitation increases from the eastern to western regions, marked by a transition from white to orange on the GSMaP.

At 08 UTC, there is a decrease in precipitation intensity in Surabaya City, with the eastern and northern parts registering 0 mm (no precipitation), while the western and southern parts have a range of 0.4-3 mm (slight precipitation). The distribution of precipitation moves southwest away from the city of Surabaya, indicated by a shift from white to green on the GSMaP. For further details, refer to Figure 10.

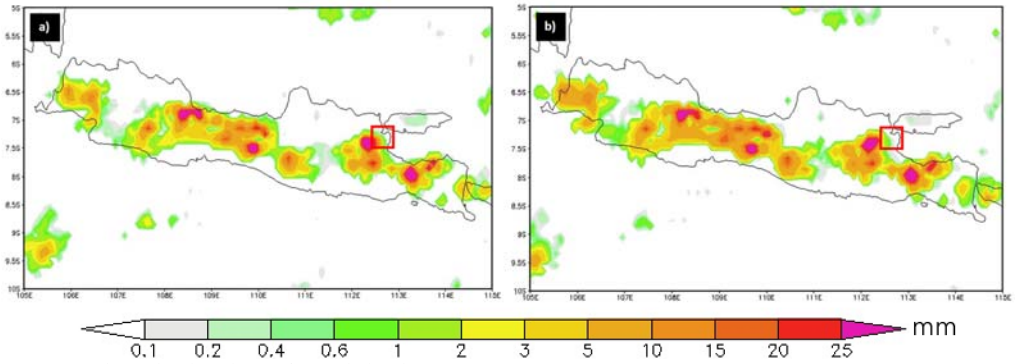

Figure 10. The Distribution of Precipitation at a) 07 UTC, b) 08 UTC

CONCLUSION

This study successfully analyzed the hail event in Surabaya using global, regional, and local meteorological parameters. Sea surface temperature anomalies in the Southeast Indian Ocean and North Java Sea contributed to large-scale atmospheric instability. Regionally, a monsoon shear line and strong low-level moisture transport from the South Java Sea indicated convergence over Surabaya. Locally, a 10% increase in relative humidity and a 3.2°C drop in surface temperature created favorable conditions for convective cloud growth. Upper-air indices such as CAPE, LI, TT, SWEAT, CIN, and KI from radiosonde data revealed moderate to high atmospheric instability, supporting hail development. Cloud tops exceeded freezing levels at 5048 m and 4776 m, with RGB Day Microphysics imagery showing overshooting tops and extremely low cloud-top temperatures reaching -82.5°C.

Three key indicators were identified as the strongest signals of hail occurrence: (1) strong convergence seen in the divergence of low-level moisture transport (LMMT), (2) moderate to high atmospheric instability, and (3) very low cloud-top temperatures below -80°C. These variables consistently aligned with the timing, location, and intensity of the hailstorm. These findings demonstrate the value of combining LMMT divergence analysis, radiosonde-derived instability indices, and satellite-based cloud-top temperature monitoring for early detection of hail potential. Integrating these indicators into forecasting systems can enhance short-term warning accuracy and help reduce hail-related risks.

REFERENCES

Abdulhakim, N. (2023). Warga Surabaya Dikagetkan dengan Fenomena Hujan Es, Temukan Butiran Es Ukuran Kecil 'Seujung Kuku'. Retrieved from https://trends.tribunnews.com/2023/03/20/warga-surabaya-dikagetkan-dengan-fenomena-hujan-es-temukan-butiran-es-ukuran-kecil-seujung-kuku

Achmad Faizal, P. K. (2023, Maret, 20). Hujan Es Terjadi di Surabaya, Ini Penjelasan BMKG. Retrieved from https://surabaya.kompas.com/read/2023/03/20/174924978/hujan-es-terjadi-di-surabaya-ini-penjelasan-bmkg

Al-Bagawi, A., Mansour, D., & Aljabri, S. (2021). Contaminations assessment of some trace metals in agricultural soil and irrigation water analysis at Hail region Saudi Arabia. *J Optoelectron Biomed Mater, 13*, 127-136.

Allen, J. T., Giammanco, I. M., Kumjian, M. R., Jurgen Punge, H., Zhang, Q., Groenemeijer, P., . . . Ortega, K. (2020). Understanding hail in the earth system. *Reviews of Geophysics, 58*(1), e2019RG000665.

Ardiansyah, D. (2022). Labilitas Atmosfer Terkait Kejadian Hujan Es (Studi Kasus Hujan Es di Sindang Dataran Bengkulu Tanggal 25 Juni 2021). *Buletin Meterologi, Klimatologi dan Geofisika, 2*(2), 34-48.

Auliya, M. N., & Mulya, A. (2022). Identifikasi Hail Berdasarkan Analisis Faktor Cuaca dan Pemanfaatan Teknik Rgb Serta Swa Pada Citra Satelit Himawari 8 (Studi Kasus: Kejadian Hujan Es di Kabupaten Malang Pada 2 Maret 2021). *Jurnal Sains & Teknologi Modifikasi Cuaca, 23*(1), 39-51.

Bao, X., & Yao, X. (2022). Intensity evolution of zonal shear line over the Tibetan Plateau in summer: A perspective of divergent and rotational kinetic energies. *Advances in Atmospheric Sciences, 39*(7), 1021-1033.

Beal, A., Hallak, R., Martins, L. D., Martins, J. A., Biz, G., Rudke, A. P., & Tarley, C. R. (2020). Climatology of hail in the triple border Paraná, Santa Catarina (Brazil) and Argentina. *Atmospheric Research, 234*, 104747.

Bessho, K., Date, K., Hayashi, M., Ikeda, A., Imai, T., Inoue, H., . . . Ohno, T. (2016). An introduction to Himawari-8/9—Japan's new-generation geostationary meteorological satellites. *Journal of the Meteorological Society of Japan. Ser. II, 94*(2), 151-183.

BMKG. (2010). *Peraturan KBMKG Nomor: Kep. 009* Jakarta.

Chakraborty, R., Basha, G., & Ratnam, M. V. (2018). Diurnal and long-term variation of instability indices over a tropical region in India. *Atmospheric Research, 207*, 145-154.

Chen, T.-C., Yen, M.-C., & Murakami, M. (1988). The water vapor transport associated with the 30–50 day oscillation over the Asian monsoon regions during 1979 summer. *Monthly weather review, 116*(10), 1983-2002.

d'Abreton, P., & Tyson, P. (1995). Divergent and non-divergent water vapour transport over southern Africa during wet and dry conditions. *Meteorology and Atmospheric Physics, 55*(1-2), 47-59.

Doty, B. E., & Kinter, J. (1995). Geophysical data analysis and visualization using the grid analysis and display system. *National Aeronautics and Space Administration, Washington, DC, USA*.

Fadholi, A. (2012). Analisa Kondisi Atmosfer pada Kejadian Cuaca Ekstrem Hujan Es (Hail). *Simetri: JurnalIlmuFisika Indonesia, 1*(2).

Fibriantika, E., & Mayangwulan, D. (2020). Analisis Spasial Indek Stabilitas Udara di Indonesia. *Jurnal Sains & Teknologi Modifikasi Cuaca, 21*(1), 1-12.

Frystine, M., Mulya, A., Kristianto, A., & Maulidyah, M. P. (2022). Analysis of Atmospheric Condition On Hail Event At Pelalawan (Case Study: September 23rd, 2019). *Jurnal Meteorologi dan Geofisika, 23*(3), 45-56.

Gold, E. (1908). The relation between wind velocity at 1000 metres altitude and the surface pressure distribution. *Proceedings of the Royal Society of London. Series A, Containing Papers of a Mathematical and Physical Character, 80*(540), 436-443.

Haryanto, Y. D., Agdialta, R., & Hartoko, A. (2020). Analisis Monsun Di Laut Jawa. *Berkala Perikanan Terubuk, 48*(2), 492-500.

Hasibuan, M. A., Shidiq, I. A., Asifin, H. A. Z., & Sa'diyah, Q. (2024). The Quantifying the Relationship Between ENSO-Induced SST Anomalies and Rainfall Variability in East Java's Coastal Regions. *Jurnal Geografi: Media Informasi Pengembangan dan Profesi Kegeografian, 21*(2), 94-102.

Hassim, M. E. E. (2012). *The influence and observability of overshooting convection in the tropical tropopause layer*: University of Melbourne, School of Earth Sciences.

Hidayat, A. M., Efendi, U., & Rahmadini, H. N. (2017). *Identifikasi Kejadian Hujan Es Berbasis Analisis Faktor Cuaca, Citra Satelit dan Model Numerik dengan Aplikasi GrADS (Studi Kasus: Kejadian Hujan Es Tanggal 19 dan 23 April 2017 di Bandung).* Paper presented at the Seminar Nasional Penginderaan Jauh ke-4.

Holton, J. R. (1992). *An Introduction to Dynamic Meteorology* (3rd Edition ed.). San Diego: Academic Press.

Houze, R. A., Jr.,. (1993). *Cloud Dynamics* (Vol. Volume 53). San Diego, USA: Academic Press.

JMA, M. S. C. M. o. (2018). *Himawari Day Microphysics RGB Quick Guide*

Jurković, P. M., Mahović, N. S., & Počakal, D. (2015). Lightning, overshooting top and hail characteristics for strong convective storms in Central Europe. *Atmospheric Research, 161*, 153-168.

Kristianto, A., Saragih, I. J. A., Larasati, G., & Akib, K. (2018). Identifikasi Kejadian Hujan Es Menggunakan Citra Radar dan Satelit Cuaca. *Proc. Pit Ke-5 Riset Kebencanaan Universitas Andalas*, 349-362.

Kunz, M., Wandel, J., Fluck, E., Baumstark, S., Mohr, S., & Schemm, S. (2020). Ambient conditions prevailing during hail events in central Europe. *Natural Hazards and Earth System Sciences, 20*(6), 1867-1887.

Lélé, M. I., Leslie, L. M., & Lamb, P. J. (2015). Analysis of low-level atmospheric moisture transport associated with the West African monsoon. *Journal of Climate, 28*(11), 4414-4430.

Lin, Y., & Kumjian, M. R. (2022). Influences of CAPE on hail production in simulated supercell storms. *Journal of the Atmospheric Sciences, 79*(1), 179-204.

McBride, J., & Keenan, T. (1982). Climatology of tropical cyclone genesis in the Australian region. *Journal of Climatology, 2*(1), 13-33.

Ni'amillah, A., Ismail, P., Siadari, E., & Saragih, I. (2021). *Study of Mesoscale Convective Complex (MCC) and its impact over the Makassar Strait (case study: 9 December 2014).* Paper presented at the IOP Conference Series: Earth and Environmental Science.

Paski, J. A. I., Permana, D. S., Sepriando, A., & Pertiwi, D. A. S. (2017). *Analisis Dinamika Atmosfer Kejadian Hujan Es Memanfaatkan Citra Radar dan Satelit Himawari-8 (Studi Kasus: Tanggal 3 Mei 2017 di Kota Bandung) Atmospheric Dynamics Analysis of Hail Event Utilizing Radar and Himawari-8 Satellite Imagery (Case Study: May 3, 2017 in Bandung City).* Paper presented at the Seminar Nasional Penginderaan Jauh.

Phoenix, D. B., & Homeyer, C. R. (2021). Simulated impacts of tropopause-overshooting convection on the chemical composition of the upper troposphere and lower stratosphere. *Journal of Geophysical Research: Atmospheres, 126*(21), e2021JD034568.

Prasetyo, S., Rumahorbo, I., Hidayat, U., & Sagita, N. (2020). *Analisis Kondisi Atmosfer pada Kejadian Hujan Es (Studi kasus: Bogor, 23 September 2020).* Paper presented at the Seminar Nasional Kahuripan.

Punge, H. J., & Kunz, M. (2016). Hail observations and hailstorm characteristics in Europe: A review. *Atmospheric Research, 176*, 159-184.

Qian, W., Leung, J. C.-H., Luo, W., Du, J., & Gao, J. (2019). An index of anomalous convective instability to detect tornadic and hail storms. *Meteorology and Atmospheric Physics, 131*, 351-373.

Sanjaya, W., & Amri, S. (2022). Analisis Citra Satelit Himawari 8/9 Terkait Kejadian Hujan Es Di Wilayah Klaten Tanggal 21 Oktober 2021. *JFT: Jurnal Fisika dan Terapannya, 9*(2), 111-119.

Schmit, T. J., Griffith, P., Gunshor, M. M., Daniels, J. M., Goodman, S. J., & Lebair, W. J. (2017). A closer look at the ABI on the GOES-R series. *Bulletin of the American Meteorological Society, 98*(4), 681-698.

Tjasyono, B. (2004). *Klimatologi* Bandung: Institut Teknologi Bandung.

Tjasyono, B. (2006). Meteorologi Indonesia 1: karakteristik dan sirkulasi atmosfer. *Badan Meteorologi dan Geofisika*.

Tokinaga, H., & Tanimoto, Y. (2004). Seasonal transition of SST anomalies in the tropical Indian Ocean during El Niño and Indian Ocean dipole years. *Journal of the Meteorological Society of Japan. Ser. II, 82*(4), 1007-1018.

Tuovinen, J.-P., Rauhala, J., & Schultz, D. M. (2015). Significant-hail-producing storms in Finland: Convective-storm environment and mode. *Weather and Forecasting, 30*(4), 1064-1076.

Wapler, K. (2017). The life-cycle of hailstorms: Lightning, radar reflectivity and rotation characteristics. *Atmospheric Research, 193*, 60-72.

Williams-Linera, G., Tolome, J., & Alvarez-Aquino, C. (2023). Hail-caused greenfall leaves, litterfall, nutrients, and leaf decomposition in tropical cloud forest and a restoration planting. *Journal of Tropical Ecology, 39*, e2.

Wirjohamidjojo, S., & Swarinoto, Y. S. (2014). *Indeks dan peredaran atmosfer tropik*: Puslitbang Badan Meteorologi, Klimatologi, dan Geofisika.

Xiu-ping, Y., Xia, Z., & Jia-li, M. (2020). Characteristics Of The Meridionally Oriented Shear Lines Over The Tibetan Plateau and Its Relationship With Rainstorms In The Boreal Summer Half-Year. *Journal of Tropical Meteorology, 26*(1).